Applied Catalysis B: Environmental 100 (2010) 510–515

Contents lists available at ScienceDirect

Applied Catalysis B: Environmental

journal homepage: www.elsevier.com/locate/apcatb

High performance Pt–Nb_2O_5/C electrocatalysts for methanol electrooxidation in acidic media

P. Justin, P. Hari Krishna Charan, G. Ranga Rao*

Department of Chemistry, Indian Institute of Technology Madras, Chennai 600 036, Tamil Nadu, India

ARTICLE INFO

Article history:
Received 10 June 2010
Received in revised form 18 August 2010
Accepted 1 September 2010
Available online 9 September 2010

Keywords:
Pt–Nb_2O_5
Methanol oxidation
Electrocatalysis
Electrooxidation
Direct methanol fuel cell

ABSTRACT

Nb_2O_5 incorporated Vulcan carbon XC-72R is prepared by solid-state reaction under intermittent microwave heating (IMH) method and the Pt nanoparticles were dispersed by microwave-assisted polyol process. The electrocatalyst samples were characterized by PXRD, TEM, XPS and the performance for methanol electrooxidation was studied in 0.5 mol L^{-1} H_2SO_4 aqueous solutions by cyclic voltammetry, chronopotentiometry and chronoamperometry. The physicochemical characterization reveals that Nb_2O_5 and Pt nanoparticles were evenly deposited on Vulcan carbon XC-72R. Electrochemical experiments showed that methanol electrooxidation performance is dependent on the amount of Nb_2O_5 loading and the peak current densities of methanol electrooxidation is significantly higher (~80%) on Pt–Nb_2O_5(2:2)/C than Pt–Ru(2:1)/C. Furthermore, Pt–Nb_2O_5(2:2)/C electrocatalyst exhibited slower current decay with time than Pt–Ru(2:1)/C, suggesting good tolerance behavior towards CO-like intermediates. The enhanced electrode response is attributed to the synergistic effect between Pt and Nb_2O_5. This work shows that Pt–Nb_2O_5/C is a promising anode catalyst for direct methanol fuel cells in terms of its activity and stability towards methanol electrooxidation.

1. Introduction

Direct methanol fuel cells (DMFCs) have emerged as one of the most promising power sources for portable electronic devices, and electric vehicles by converting chemical energy directly into electrical energy in an environmentally friendly manner [1,2]. The operation of DMFCs involves methanol electrooxidation at anode and the oxygen reduction at cathode over precious metal catalysts dispersed on a carbon support. The Pt and/or Pt–Ru based catalysts are employed as anodes in standard DMFC devices because of their excellent performance in catalyzing the dehydrogenation of methanol, a key step in the direct oxidation of methanol to CO_2 [3]. Unlike hydrogen, the production, purification, storage, distribution, and utilization of liquid methanol is very simple, and does not need extensive modification of the existing fuel infrastructure. Moreover, the energy density of liquid fuels such as methanol (5 kWh L^{-1}) is much higher than gaseous fuels such as hydrogen (0.53 kWh L^{-1}) at 20 MPa [2]. Despite these advantages, high overpotentials for methanol electrooxidation and methanol crossover from anode to cathode through a membrane prevent the use of DMFCs for practical applications. Carbon monoxide generated from the incomplete oxidation of methanol invariably binds strongly to the Pt anode as a poison. The removal of adsorbed CO requires high overpotentials, a challenging task which is addressed by alloying Pt with other metals or adding small amounts of catalytically active oxide materials. The magnitude of methanol electrooxidation current is enhanced at Pt electrode by alloying it with co-catalysts such as Ru [4–6], Sn [7], W [8], Mo [9], Rh [10], Os [11] and Au [12] which promote CO electrooxidation. So far, PtRu alloy has been found to be the most active binary catalyst in which Ru generates surface oxygen containing species at lower potentials to oxidize CO to CO_2 [3]. The enhanced activity of PtRu is originally explained by bifunctional mechanism [13] and ligand (or electronic) effect [14]. The electrocatalytic activity of PtRu particles is also sensitive to the structure, composition, particle size, morphology and degree of PtRu alloying. Multi-component catalysts show superior performance than Pt but prohibitively expensive for fuel cell applications [4–12].

Recently, metal oxide promoted Pt electrocatalysts have been considered for direct electrooxidation of methanol in acidic [15,16] as well as in alkaline media [17]. Metal oxides with good catalytic properties and having stronger interaction with Pt nanoparticles can generate active interfacial regions in the electrocatalysts and enhance the catalytic activity towards methanol electrooxidation. The Pt nanoparticles incorporated in metal oxides such as, CeO_2 [15,16], MoO_x [18], TiO_2 [19], SnO_2 [20], RuO_2 [21], WO_3 [22], sulfated ZrO_2 [23], and MnO_2 [24], have been pursued as potential catalysts in acidic media in order to increase the electrocatalytic activity and stability. This approach reduces the poisoning effects

* Corresponding author. Tel.: +91 44 2257 4226; fax: +91 44 2257 0545.
E-mail address: grrao@iitm.ac.in (G. Ranga Rao).

0926-3373/$ – see front matter © 2010 Elsevier B.V. All rights reserved.
doi:10.1016/j.apcatb.2010.09.001

and the amount of noble metal required in the composite electrode. The oxide support is believed to stabilize Pt particle dispersion and modify their electronic property as well [25]. Moreover, they possess oxygen storage and release property, which plays an important role in CO electrooxidation mechanism [15,16]. The composite electrode materials containing metal oxides are expected to promote the activity of electrooxidation of methanol by supplying required amount of oxygen and enhancing the CO tolerance.

The *n*-type Nb_2O_5 semiconductor (3.4 eV band-gap) is remarkable material having applications in catalysis [25,26], optical [27], field emission [28], lithium ion batteries [29] electrochromic devices [30] and photovoltaic cells [31] because of its excellent microtextural properties, high refractive index, chemical stability, and corrosion resistance properties. Recently Orilall et al. [32] employed one-pot synthesis of Pt and Pt–Pb nanoparticles incorporated into mesoporous niobium oxide–carbon composites for formic acid electrooxidation. This study shows an onset potential shift of 60 mV less positive and a mass activity four times higher than the best reported values for PtPb intermetallic nanoparticles for formic acid electrooxidation. In the present work, the Nb_2O_5/C composites are prepared by solid-state reaction under intermittent microwave heating (IMH) method and Pt nanoparticles are dispersed over Nb_2O_5/C composites by microwave-assisted polyol process. Nb_2O_5 promotes the electrocatalytic activity and poison resistance behavior of Pt/C catalysts for methanol electrooxidation in acidic media.

2. Experimental

2.1. Preparation of composite electrocatalysts

The Nb_2O_5/C composites were prepared by solid-state reaction under intermittent microwave heating (IMH) method. Nb_2O_5 (Alfa Aesar, purity = 99.9%) was well dispersed over Vulcan XC-72R (C) carbon black (Cabot Corp., $S_{BET} = 250\ m^2\ g^{-1}$) using 2-propanol as solvent by ultrasonic treatment for 15 min and the mixture was dried in an oven at 80 °C. It was then introduced into a microwave oven (Sharp NN-S327 WF, 2450 MHz, and 1100 W) and heated in six cycles, each cycle for 20 s with a pause of 60 s between heating cycles. Pt nanoparticles were dispersed over Nb_2O_5/C by microwave-assisted polyol process [33]. Typically 0.5 mL of 0.1 mol L^{-1} $H_2PtCl_6{\cdot}6H_2O$ (Aldrich, A.C.S. Reagent) was mixed with 25 mL of ethylene glycol (AR grade) in 100 mL beaker. 0.4 mol L^{-1} KOH (in ethylene glycol) was added drop wise to adjust the solution pH to about 10 in order to induce the formation of small and uniform Pt nanoparticles. This mixture was sonicated after adding 0.045 g, 0.05 g and 0.055 g of Nb_2O_5/C composites for preparing Pt–Nb_2O_5(2:1)/C, Pt–Nb_2O_5(2:2)/C and Pt–Nb_2O_5(2:3)/C catalyst respectively and the mixtures were subjected to microwave irradiation for 50 s. The resulting suspension was filtered and the residue was washed with acetone and dried at 35 °C in a vacuum oven overnight. For comparative studies, commercial Pt–Ru(2:1)/C catalyst (Johnson Matthey) was used. The amounts of Vulcan XC-72R carbon and Pt in each sample are 0.04 g and 0.01 g respectively.

2.2. Physical characterization

The phases and lattice parameters of the composite catalysts were characterized by powder X-ray diffraction (PXRD) employing Bruker AXS D8 diffractometer with Cu Kα radiation (λ = 0.15418 nm) operating at 40 kV and 30 mA. The average crystallite size of the Pt particles is estimated using the Scherrer equation, $D = 0.9\lambda/(\beta\cos\theta)$ where D is the crystallite size, λ is the wavelength of the incident X-ray, θ is the diffraction angle for (2 2 0) peak and β is the full width at half maximum (FWHM) of peaks measured graphically. X-ray photoelectron spectroscopy (XPS) measurements were performed on Omicron Nanotechnology spectrometer with Mg Kα monochromatic source operating at 15 kV and 20 mA. The spectra were recorded using 25 eV analyzer pass energy. High-resolution TEM (HRTEM) characterization was performed with a JEOL JEM-3010 transmission electron microscopy (TEM) operated at 200 kV. Samples for HRTEM analysis were prepared by drying the nanocrystal dispersion in acetone on amorphous carbon-coated copper grids.

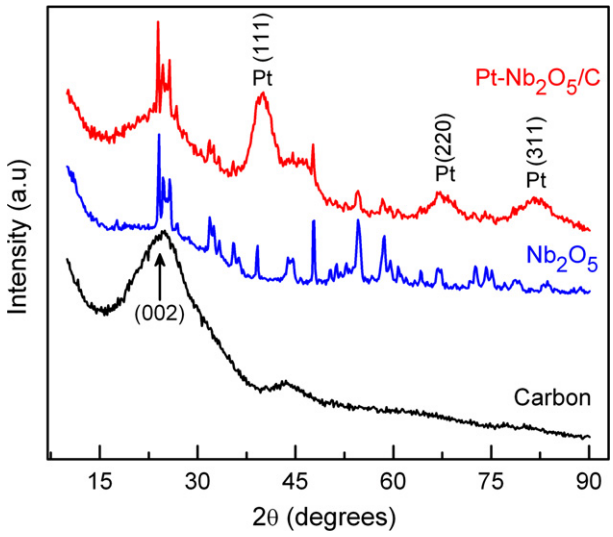

Fig. 1. Powder XRD pattern of Vulcan XC-72R, Nb_2O_5 and Pt–Nb_2O_5(2:2)/C.

2.3. Electrochemical characterization

The working electrodes for electrochemical measurements were fabricated by dispersing Pt–Ru/C or Pt–Nb_2O_5/C powders in 1.0 mL of distilled water and 0.1 mL of 5 wt% Nafion. Ultrasonic treatment was given for 15 min to achieve uniform dispersion of the mixture at room temperature. A known amount of suspension was deposited on the surface of a glassy carbon electrode (area = 0.28 cm^{-2}) and the solvent was slowly evaporated. The Pt loadings on Pt–Ru/C and Pt–Nb_2O_5/C electrodes were normally controlled at 0.21 mg cm^{-2}. Electrochemical measurements were carried out in a conventional three electrode cell using CHI 7081C electrochemical workstation. A platinum foil and Ag/AgCl (BAS Instruments, USA) were used as counter and reference electrodes respectively. The test solution consists of 0.5 mol L^{-1} H_2SO_4 and 1 mol L^{-1} CH_3OH. The dissolved oxygen was removed by purging the solution with pure nitrogen for 30 min before starting the electrochemical experiments.

3. Results and discussion

3.1. Microstructure studies

The powder XRD patterns of Vulcan XC-72R (C), Nb_2O_5 and Pt–Nb_2O_5(2:2)/C catalysts are shown in Fig. 1. A typical broad diffraction peak for hexagonal Vulcan carbon XC-72R is observed at 24.8° due to (0 0 2) reflection. The peaks and the corresponding reflections at $2\theta = 40.1°$ (1 1 1), 46.6° (2 0 0), 68.1° (2 2 0) and 81.7° (3 1 1) are indexed to the face-centered cubic structure of Pt crystallites present in the Pt–Nb_2O_5(2:2)/C catalyst samples [5,7,16]. The peak at $2\theta = 40.1°$ is broad and intense, which indicates that the Pt particles are essentially orientated towards Pt(1 1 1) plane. The Pt(1 1 1) plane contains hexagonally packed Pt atoms and does not undergo surface reconstruction, unlike Pt(1 0 0) and Pt(1 1 0)

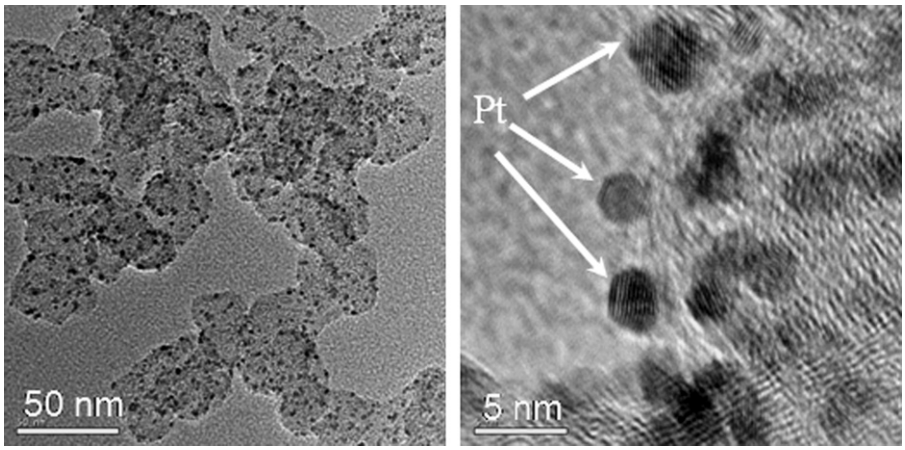

Fig. 2. TEM images of Pt–Nb_2O_5(2:2)/C with different magnifications.

surfaces. Chrzanowski et al. reported that the (1 1 1) plane of Pt is stable and the most active surface towards methanol oxidation [34]. The XRD peaks corresponding to Pt particles are superimposed on Nb_2O_5 reflections at $2\theta = 23.7^\circ$, 32.1°, 47.64°, 54.6° and 58.1°. The other weak reflection of Pt particles at 68.1° is also very broad which confirms that the size of the Pt particles is in the nano-range. The (2 2 0) peak of Pt fcc structure at $2\theta = \sim 68.1^\circ$ has been used for calculating the mean crystallite size to avoid the interference of the broad signal from the carbon support [6]. The mean crystallite size of Pt particles obtained is 2.7 nm. Fig. 2 shows the TEM images of homogeneously dispersed spherical Pt metal particles (dark spots) of about 2–3 nm size embedded in the Nb_2O_5/C support. In general, there is a homogeneous distribution of Pt particles with some agglomeration which is a characteristic of oxide incorporated samples [7,15,17]. The homogeneous microwave heating of liquid samples has an advantage of reducing the temperature and concentration gradients in the reaction medium, providing uniform environment for the nucleation and growth of the metal nanoparticles [33]. Rapid heating by microwave accelerates the reduction of metal ions and the nucleation of metal particles in the presence of ethylene glycol as a reducing agent. In our catalyst preparation, the precursor solution contains 400 mg/L (ppm) of Pt metal (i.e., 25 mL of ethylene glycol contains 0.5 mL of 0.1 mol L^{-1} $H_2PtCl_6{\cdot}6H_2O$ = 10 mg of Pt). But filtrate solution contains only 0.142 mg/L (ppm) of Pt as identified by inductively coupled plasma mass spectrometry (ICP-MS) analysis. This essentially means that ~99.96% of Pt is loaded on the Nb_2O_5/C material. So deviation from the theoretical value is only marginal (~0.04%). This is the one of the advantages of the microwave-assisted polyol process in addition to rapid (50 s) and more efficient way of obtaining uniform metal particle deposition on the support [7,15,17,33].

The XPS analysis of Pt–Nb_2O_5/C catalyst samples in the Pt 4f and Nb 3d regions are presented in Fig. 3. The Pt 4f region displays the spin-orbit splitting doublet peaks of $4f_{7/2}$ and $4f_{5/2}$ [35]. Deconvo-

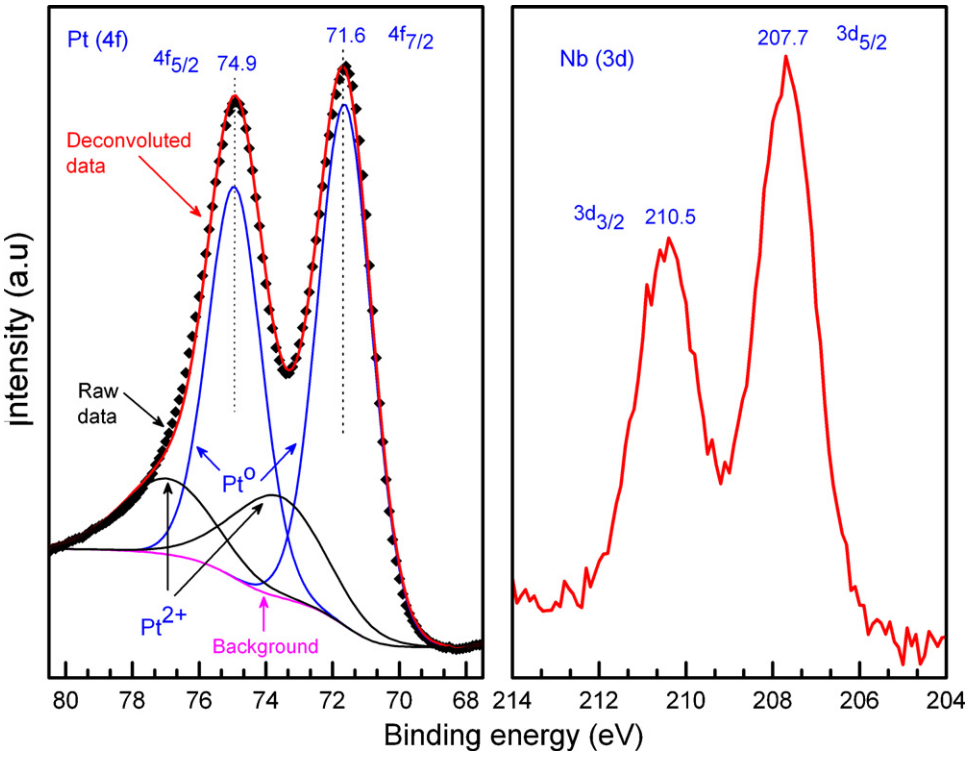

Fig. 3. Pt 4f and Nb 3d photoemission spectra of Pt–Nb_2O_5(2:2)/C electrocatalyst.

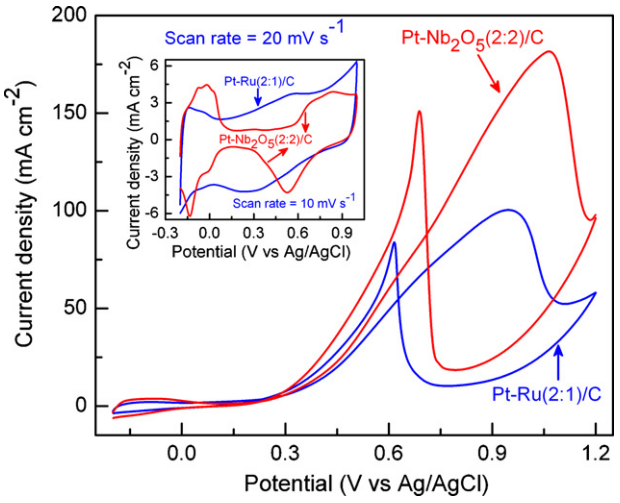

Fig. 4. Cyclic voltammograms for electrooxidation of methanol on Pt–Ru/C and Pt–Nb_2O_5(2:2)/C electrodes in N_2 saturated solution of 1.0 mol L^{-1} CH_3OH in 0.5 mol L^{-1} H_2SO_4 at a scan rate of 20 mV s^{-1}. Inset shows the hydrogen electroadsorption voltammetric profiles of Pt–Ru/C and Pt–Nb_2O_5(2:2)/C electrodes in N_2 saturated solution of 0.5 mol L^{-1} H_2SO_4 at a scan rate of 10 mV s^{-1}.

lution of Pt 4f region shows the presence of two pairs of doublets with theoretical peak area ratio of 57:43. The more intense doublet peaks at 71.6 eV and 74.9 eV are attributed to metallic Pt. The second and weaker doublet at 73.5 eV and 76.9 eV with higher binding energy (BE) of 1.9 eV than that of Pt^0 could be assigned to Pt^{2+} species due to surface oxide/hydroxide [5,36,37]. The relative area of integrated peak intensities of Pt^0 peak is 75% higher than that of Pt^{2+} species (25%) which is comparable [5] or better [36] than the reported ratios in the literature. This means that the surface of Pt particles is predominately in the Pt^0 state. Curve fitting of the Pt $4f_{7/2}$ also reveals a positive shift of 0.5 eV for $4f_{7/2}$ peak towards higher binding energy compared to that of pure element [35]. This positive shift of 0.5 eV is due to the induced positive charge on the dispersed Pt particles interacting with the oxide support [37–39]. A pair of peaks due to the Nb 3d core level split is observed at binding energies of 210.5 eV and 207.7 eV which correspond to the +5 ionic state of niobium in the oxide support. The XRD, XPS and TEM results confirm that there is an active interface between embedded Pt particles and Nb_2O_5 support in the Pt–Nb_2O_5/C electrocatalyst.

3.2. Electrochemical studies

3.2.1. Cyclic voltammetry

The cyclic voltammograms recorded in 1.0 mol L^{-1} CH_3OH/0.5 mol L^{-1} H_2SO_4 aqueous solution at a scan rate of 20 mV s^{-1} are shown in Fig. 4. The Faradaic current exhibits the well-known dependence on the electrode potential typical for the methanol electrooxidation reaction in acidic media on a Pt containing carbon catalyst [7,16,18,20,23,40,41]. The peak current densities for Pt–Ru(2:1)/C and Pt–Nb_2O_5(2:2)/C electrodes are about 101 mA cm^{-2} and 183 mA cm^{-2} respectively. The CO species are generated on the catalyst surface due to incomplete oxidation of methanol [40]. The higher increment in methanol electrooxidation activity of Pt–Nb_2O_5(2:2)/C electrode is attributed to faster removal of CO, facilitating methanol adsorption on fresh and regenerated Pt sites in the presence of Nb_2O_5. This observation is in agreement with the results reported in the literature on the other metal oxides promoted electrocatalysts for methanol electrooxidation [15,16,20,24]. Therefore using the same amount of Pt, higher electrocatalytic currents are obtained in the case of Pt–Nb_2O_5(2:2)/C electrode. A catalyst for methanol oxidation should be able to break C–H and O–H bonds of methanol and facilitate the reaction of the resulting residue with some O-containing species to form CO_2 [13,14]. This leads to the formation of strongly adsorbed linearly bound surface CO species leading to self-poisoned Pt catalyst. The surface oxygen of a reducible oxide helps oxidizing the adsorbed CO on Pt surface and the oxide surface is replenished by redox reaction with water [15,16,18,22,24]. The importance of surface oxygen source for the effective CO oxidation at lower potentials in DMFC electrocatalyst has been highlighted recently in the case of cobalt oxides samples [42]. Nb_2O_5 is a well-known reducible oxide which shows high oxygen storage capacity and strong metal support interaction between Pt and Nb_2O_5 [25,30,43]. We propose the following reaction mechanism for methanol electrooxidation on Pt–Nb_2O_5/C catalysts:

$$Nb_2O_5 + H_2O \rightarrow Nb_2O_5\text{–}OH_{ads} + H^+ + e^- \quad (1)$$

$$Pt\text{–}CO_{ads} + Nb_2O_5\text{–}OH_{ads} \rightarrow Pt + Nb_2O_5 + CO_2 + H^+ + e^- \quad (2)$$

$$Pt \ldots Nb_2O_5(\text{interface}) + xCO \rightarrow Pt \ldots Nb_2O_{5-x}(\text{interface}) + xCO_2 \quad (3)$$

The enhancement of methanol oxidation is likely to occur at the interface of Pt and Nb_2O_5 in the supported system. In the presence of Nb_2O_5 as promoter, water adsorption starts at lower potential at the interface of Pt...Nb_2O_5 thereby reducing the anodic overpotentials. The Pt–CO species is oxidized to CO_2 at the Pt...Nb_2O_5 interface. The cyclic voltammograms of Pt–Nb_2O_5(2:2)/C and Pt–Ru(2:1)/C catalysts in 0.5 mol L^{-1} H_2SO_4 solution at a scan rate of 10 mV s^{-1} are shown in the inset of Fig. 4. The Pt–Nb_2O_5/C shows electrocatalytic activity typical of Pt electrode in acidic electrolytes. The peaks for hydrogen adsorption and desorption ($-0.2\,V \le E \le 0.1\,V$), the double layer potential plateau, and the peaks due to the formation (0.5–1.0 V) and reduction (1.0–0.25 V) of platinum surface oxides are well defined [18,20]. In the case of Pt–Ru(2:1)/C, the voltammetric profile shows enlarged double layer region which is a typical response of the Pt–Ru electrode in acid electrolytes [4,6,44]. Hydrogen adsorption and desorption features are present in the voltammetric profiles of Pt–Ru(2:1)/C but diminished relative to pure Pt reflecting the incorporation of Ru. The broadening of double layer region and the inhibition of classical hydrogen adsorption peaks occur from the pseudocapacitive contribution to the double layer charging currents of Ru alloyed or segregated as a metal or oxide [6].

The amount of Nb_2O_5 in Pt–Nb_2O_5/C composites has a significant role to play in the electrocatalytic activity for methanol electrooxidation. Cyclic voltammetry studies have been performed in order to determine the optimum ratio of Pt/Nb_2O_5 composites on methanol electrooxidation by fixing platinum loading to 0.21 mg cm^{-2}. Fig. 5 shows that the peak current density increases with Nb_2O_5 content and at the same time the onset potential is shifted more towards negative side. The best performance is found when Nb_2O_5 loading is about 0.21 mg cm^{-2}, or the weight ratio of Pt and Nb_2O_5 is 2:2 (Table 1). Further increase in Nb_2O_5 content diminishes the electrode conductivity and also affects its performance due to the inhibition of methanol adsorption on Pt sites. Furthermore, the catalytic current of Pt–Nb_2O_5(2:2)/C electrode begins to rise sharply at more negative potential which can contribute substantially to the overall cell efficiency.

3.2.2. Chronopotentiometry

Chronopotentiometry is a powerful tool to study the anti-poisoning abilities of electrocatalysts for methanol electrooxidation [45]. The change in electrode potential with time recorded for all the electrodes at fairly high bias current of 7.5 mA cm^{-2} are illustrated in Fig. 6. For all electrodes, there is a slow increase

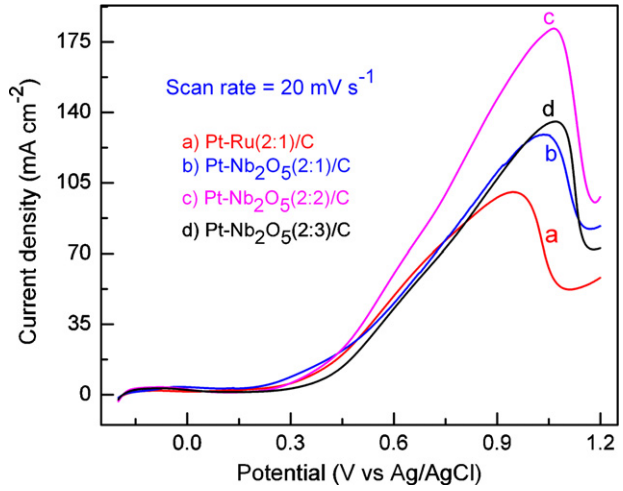

Fig. 5. Cyclic voltammograms for electrooxidation of methanol on Pt–Ru/C and Pt–Nb_2O_5/C electrodes with various amounts of Nb_2O_5 in N_2 saturated solution of 1.0 mol L^{-1} CH_3OH in 0.5 mol L^{-1} H_2SO_4 at a scan rate of 20 mV s^{-1}. For clarity only forward scans are shown here. Pt loading = 0.21 mg cm^{-2}.

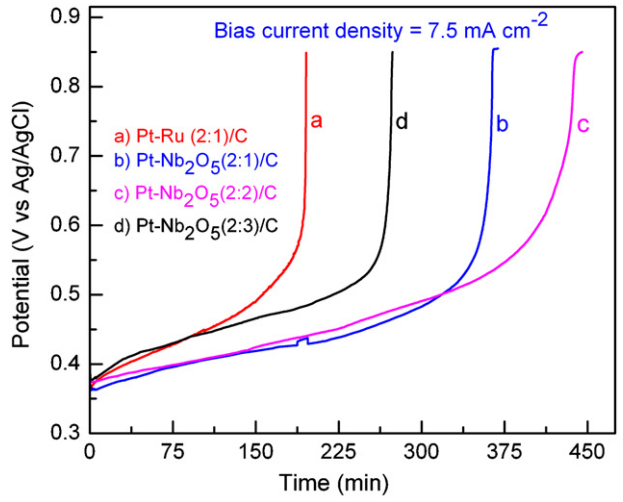

Fig. 6. Chronopotentiometric curves of methanol electrooxidation on various electrodes at current density of 7.5 mA cm^{-2}.

in electrode potential with polarization time before a steep rise in potential which indicates the loss of methanol electrooxidation activity favoring the oxygen evolution. This is due to the fact that during the chronopotentiometric experiment, the poisonous species, mainly CO_{ads} generated from methanol electrooxidation, are accumulated on the Pt surface of electrocatalysts and thereby inhibiting further the methanol electrooxidation reaction. When

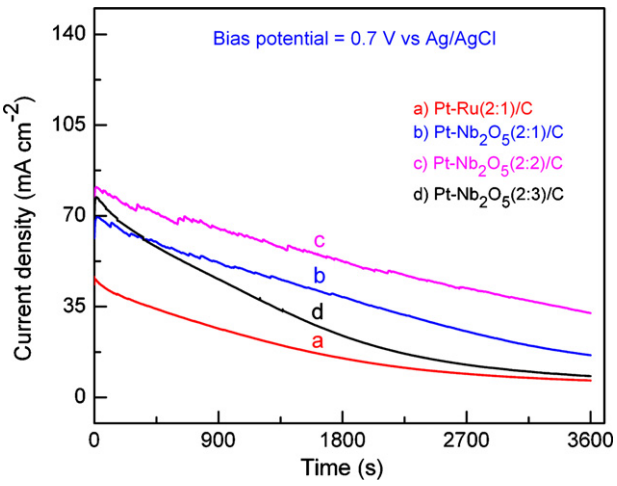

Fig. 7. Chronoamperometry curves of methanol electrooxidation on various electrodes at bias potential of 0.7 V with respect to Ag/AgCl.

the electrodes are poisoned deeply, the methanol electrooxidation cannot continue. To satisfy the applied anodic current density, the potential must jump to a higher potential, at which water is decomposed [45,46]. The polarization potentials are relatively lower for Pt–Nb_2O_5(2:2)/C electrode because the catalyst can withstand against poisoning species for longer time than Pt–Ru(2:1)/C. For example, the Pt–Ru(2:1)/C electrode reaches 0.55 V within 183 min while Nb_2O_5 incorporated Pt catalysts are more stable for much longer periods. The optimum Pt–Nb_2O_5(2:2)/C electrode retains its electrocatalytic activity two times longer than the Pt–Ru(2:1)/C at 0.55 V (Table 1).

3.2.3. Chronoamperometry

The electrochemical stability of all four electrodes for methanol electrooxidation is investigated by chronoamperometric experiments at bias potential of 0.7 V with respect to Ag/AgCl reference electrode in 1.0 mol L^{-1} CH_3OH/0.5 mol L^{-1} H_2SO_4 electrolyte at room temperature for 3600 s. The results are presented in Fig. 7. The polarization current for the methanol electrooxidation reaction shows a decay with time analogous to the methanol electrooxidation reaction on the Pt-based electrocatalysts in acid media [6,16,22,23,34]. But, both the initial and limiting current densities of Pt–Nb_2O_5(2:1)/C and Pt–Nb_2O_5(2:2)/C electrodes are much higher than those obtained for Pt–Ru/C electrode in the entire time range. For Pt–Ru/C electrode, the potentiostatic current decreases to 35 mA cm^{-2} in 420 s, while a Pt–Nb_2O_5(2:2)/C electrode retains the same current density for about 3400 s. The higher stability of Pt–Nb_2O_5(2:2)/C catalysts in comparison with that of Pt–Ru/C catalyst at 0.7 V bias potential indicates considerable improvement in poison tolerance mechanism, and hence an increase in the stability of the catalyst with Nb_2O_5 acting as a promoter. This

Table 1
Evaluation of electroactivity and stability of methanol electrooxidation on various electrode materials.

Electrode	i_p[a] (mA cm^{-2})	Stability			
		By chronopotentiometry (time in min at 0.55 V)	By chronoamperometry		
			Current at 300 s (mA cm^{-2})	Current at 1800 s (mA cm^{-2})	% Decrease in activity after 1800 s
Pt–Ru(2:1)/C	101	183	36.8	15.0	59
Pt–Nb_2O_5(2:1)/C	129	345	61.6	38.9	37
Pt–Nb_2O_5(2:2)/C	183	378	72.0	52.6	27
Pt–Nb_2O_5(2:3)/C	136	259	63.5	23.6	63

[a] Peak current density from cyclic voltammetry.

observation is further corroborated by the small current spikes observed on the potentiometric curves of Pt–Nb_2O_5(2:1)/C and Pt–Nb_2O_5(2:2)/C electrodes which are absent on the potentiometric curves of Pt–Nb_2O_5(2:3)/C and Pt–Ru/C electrodes (Fig. 7). The current spikes are due to the detachment of the CO_2 product bubbles formed on the electrode surface. These bubbles hinder the diffusion of the reactant to the electrode surface. When they detach, they cause local stirring and replenish the electrolyte adjacent to the electrode which produces a jump in the methanol oxidation current [47].

4. Conclusions

In summary, Nb_2O_5 have been incorporated on Vulcan carbon XC-72R by a novel low-cost, reproducible, intermittent microwave heating (IMH) method. Combining the results from the cyclic voltammetry, chronopotentiometry and chronoamperometric experiments, we conclude that Pt–Nb_2O_5/C electrocatalysts are excellent anode materials for direct methanol fuel cells in terms of their activity and stability. There is a significant enhancement in electrocatalytic activity for methanol electrooxidation which can be attributed to the strong metal support interactions observed between Pt and Nb_2O_5 [25]. It is possible to enhance the electrocatalytic activity further by increasing the specific surface area of Nb_2O_5 with suitable pore-size distribution. The approach described in this study is suitable for the incorporation of other oxides directly onto the conducting carbon, thus opening the door to develop oxide-supported Pt electrocatalysts within a short span of time.

Acknowledgments

We thank the Ministry of New and Renewable Energy, Government of India, for the financial support through Project No. 102/28/2006-NT.

References

[1] S. Wasmus, A. Küver, J. Electroanal. Chem. 461 (1999) 14–31.
[2] S.K. Kamarudin, W.R.W. Daud, S.L. Ho, U.A. Hasran, J. Power Sources 163 (2007) 743–754.
[3] H. Liu, C. Song, L. Zhang, J. Zhang, H. Wang, D.P. Wilkinson, J. Power Sources 155 (2006) 95–110.
[4] R. Basnayake, Z. Li, S. Katar, W. Zhou, H. Rivera, E.S. Smotkin, D.J. Casadonte, C. Korzeniewski, Langmuir 22 (2006) 10446–10450.
[5] N.-Y. Hsu, C.-C. Chien, K.-T. Jeng, Appl. Catal. B: Environ. 84 (2008) 196–203.
[6] D.R.M. Godoi, J. Perez, H.M. Villullas, J. Phys. Chem. C 113 (2009) 8518–8525.
[7] Z. Liu, B. Guo, L. Hong, T.H. Lim, Electrochem. Commun. 8 (2006) 83–90.
[8] M. Umeda, H. Ojima, M. Mohamedi, I. Uchida, J. Power Sources 136 (2004) 10–15.
[9] S. Mukerjee, R.C. Urian, Electrochim. Acta 47 (2002) 3219–3231.
[10] J.H. Choi, K.W. Park, I.S. Park, W.H. Nam, Y.E. Sung, Electrochim. Acta 50 (2004) 787–790.
[11] J.T. Moore, D. Chu, R. Jiang, G.A. Deluga, C.M. Lukehart, Chem. Mater. 15 (2003) 1119–1124.
[12] Y.Q. Wang, Z.D. Wei, L. Li, M.B. Ji, Y. Xu, P.K. Shen, J. Zhang, H. Zhang, J. Phys. Chem. C 112 (2008) 18672–18676.
[13] M. Watanabe, S. Motoo, J. Electroanal. Chem. 60 (1975) 267–273.
[14] T. Frelink, W. Visscher, J.A.R. van Veen, Surf. Sci. 335 (1995) 353–360.
[15] J. Wang, J. Xi, Y. Bai, Y. Shen, J. Sun, L. Chen, W. Zhu, X. Qiu, J. Power Sources 164 (2007) 555–560.
[16] M.A. Scibioh, S.K. Kim, E.A. Cho, T.H. Lim, S.A. Hong, H.Y. Ha, Appl. Catal. B: Environ. 84 (2008) 773–782.
[17] P. Justin, G. Ranga Rao, Catal. Today 141 (2009) 138–143.
[18] Y. Wang, E.R. Fachini, G. Cruz, Y. Zhu, Y. Ishikawa, J.A. Colucci, C.R. Cabrera, J. Electrochem. Soc. 148 (2001) C222–C226.
[19] K.W. Park, S.B. Han, J.M. Lee, Electrochem. Commun. 9 (2007) 1578–1581.
[20] M.S. Saha, R. Li, M. Cai, X. Sun, Electrochem. Solid-State Lett. 10 (2007) B130–B133.
[21] L. Cao, F. Scheiba, C. Roth, F. Schweiger, C. Cremers, U. Stimming, H. Fuess, L. Chen, W. Zhu, X. Qiu, Angew. Chem. Int. Ed. 45 (2006) 5315–5319.
[22] B. Rajesh, K.R. Thampi, J.M. Bonard, N. Xanthopoulos, H.J. Mathieu, B. Viswanathan, J. Phys. Chem. B 107 (2003) 2701–2708.
[23] D.-J. Guo, X.-P. Qiu, W.-T. Zhu, L.-Q. Chen, Appl. Catal. B: Environ. 89 (2009) 597–601.
[24] C. Zhou, H. Wang, F. Peng, J. Liang, H. Yu, J. Yang, Langmuir 25 (2009) 7711–7717.
[25] P. Marques, N.F.P. Ribeiro, M. Schmal, D.A.G. Aranda, M.M.V.M. Souza, J. Power Sources 158 (2006) 504–508.
[26] D.E. Keller, S.M.K. Airaksinen, A.O. Krause, B.M. Weckhuysen, D.C. Koningsberger, J. Am. Chem. Soc. 129 (2007) 3189–3197.
[27] C.C. Lee, C.L. Tien, J.C. Hsu, Appl. Opt. 41 (2002) 2043–2047.
[28] B. Varghese, S.C. Haur, C.-T. Lim, J. Phys. Chem. C 112 (2008) 10008–10012.
[29] A.L. Viet, M.V. Reddy, R. Jose, B.V.R. Chowdari, S. Ramakrishna, J. Phys. Chem. C 114 (2010) 664–671.
[30] R. Romero, E.A. Dalchiele, F. Martín, D. Leinen, J.R. Ramos-Barrado, Sol. Energy Mater. Sol. Cells 93 (2009) 222–229.
[31] J. Lee, M.C. Orilall, S.C. Warren, M. Kamperman, F.J. Disalvo, U. Wiesner, Nat. Mater. 7 (2008) 222–228.
[32] M.C. Orilall, F. Matsumoto, Q. Zhou, H. Sai, H.D. Abruña, F.J. DiSalvo, U. Wiesner, J. Am. Chem. Soc. 131 (2009) 9389–9395.
[33] W.X. Chen, J.Y. Lee, Z. Liu, Chem. Commun. (2002) 2588–2589.
[34] W. Chrzanowski, H. Kim, A. Wieckowski, Catal. Lett. 50 (1998) 69–75.
[35] S. Hüfner, Photoelectron Spectroscopy: Principles and Applications, Springer, Heidelberg, 1996.
[36] F. Liu, J.Y. Lee, W. Zhou, Adv. Funct. Mater. 15 (2005) 1459–1464.
[37] D.-H. Lim, D.-H. Choi, W.-D. Lee, H.-I. Lee, Appl. Catal. B: Environ. 89 (2009) 484–493.
[38] B.A. Pereira, F. Laplante, M. Chaker, D. Guay, Adv. Funct. Mater. 17 (2007) 443–450.
[39] A. Kongkanand, K. Vinodgopal, S. Kuwabata, P.V. Kamat, J. Phys. Chem. B Lett. 110 (2006) 16185–16188.
[40] T.C. Deivaraj, J.Y. Lee, J. Power Sources 142 (2005) 43–49.
[41] M. Nogami, R. Koike, R. Jalem, G. Kawamura, Y. Yang, Y. Sasaki, J. Phys. Chem. Lett. 1 (2010) 568–571.
[42] E. Antolini, J.R.C. Salgado, E.R. Gonzalez, Appl. Catal. B: Environ. 63 (2006) 137–149.
[43] H.-J. Chun, D.B. Kim, D.-H. Lim, W.-D. Lee, H.-I. Lee, Int. J. Hydrogen Energy 35 (2010) 6399–6408.
[44] D. Chu, S. Gilman, J. Electrochem. Soc. 143 (1996) 1685–1690.
[45] M. Krausa, W. Vielstich, J. Electroanal. Chem. 399 (1995) 7–12.
[46] J. Chen, M. Wang, B. Liu, Z. Fan, K. Cui, Y. Kuang, J. Phys. Chem. B 110 (2006) 11775–11779.
[47] J. Jiang, A. Kucernak, J. Electroanal. Chem. 543 (2003) 187–199.